Ceramics-Silikáty 66 (4), 471-479 (2022)
www.ceramics-silikaty.cz doi: 10.13168/cs.2022.0043

PREPARATION AND THERMAL-MECHANICAL PROPERTIES OF ALUMINUM TITANATE BASED CERAMICS

HONGQUAN ZHANG*, ZHIYONG PENG*, #JIN WEN*, PENGJIE CHEN**, FENGSHENG LIN*

*School of Materials Science and Engineering, Wuhan University of Technology, Wuhan 430070, PR China
**Jieyang Hengcheng Ceramic Technology Co. Ltd., Jieyang 522021, PR China

#E-mail: wen9888@Hotmail.com

Submitted August 16, 2022; accepted September 19, 2022

Keywords: Al_2TiO_5 solid solution, Low thermal expansion, Thermal shock resistance, CaO additive

Aluminium titanate (Al_2TiO_5) based ceramic materials were successfully processed through the addition of porcelain clay and different amounts of CaO to the stoichiometric alumina - titania mixtures that contained commonly used MgO and Fe_2O_3 additives at 1350 - 1400 °C for 1 h. The effect of the addition of CaO and sintering temperatures on the formation of the Al_2TiO_5 ceramics and thermal-mechanical performances were investigated. The results revealed that CaO promoted the formation of a long columnar Al_2TiO_5 solid solution and anorthite as well as gahnite phases. Due to the mismatch of the thermal expansion coefficient between the Al_2TiO_5 solid solution crystals and the anorthite and gahnite phases, a compressive residual stress developed on the surface of the Al_2TiO_5 solid solution particulates, effectively improving the mechanical properties and inhibiting the thermal decomposition of the Al_2TiO_5 solid solution and the microcrack propagation. The average thermal expansion coefficient (20 - 800 °C) of the sample with 3 wt. % CaO sintered at 1400 °C for 60 min was 0.80×10^{-6} °C^{-1}, and the flexural strength of the sample with 5 wt. % CaO sintered at 1380 °C was as high as 58.59 MPa, with a 12.43 % increase in the strength after the thermal shock test.

INTRODUCTION

Aluminium titanate (Al_2TiO_5: AT) has a very low coefficient of thermal expansion ($0.2 - 1.5 \times 10^{-6}$ °C^{-1}) and a high melting point (1860 °C), exhibiting extremely good thermal shock resistance and low thermal conductivity ($0.9 - 1.5$ W·m^{-1}·°C^{-1}) [1 - 3], which make it most suitable to be an excellent heat-resistant and thermal shock-resistant material in a variety of high-temperature ceramic parts and in various lining parts of the non-ferrous metal industry [4]. However, considerable inter-granular microcracking occurring due to the high thermal anisotropy of the individual grains and the thermal decomposition generated at the temperatures of about 750 − 1280 °C greatly weaken the mechanical properties of the polycrystalline Al_2TiO_5 and limit their application [5, 6]. Many attempts have been made so far to improve its thermal stability and depress the thermal decomposition. It has been reported that the above limitations could be resolved by the formation of stable solid solutions and through the microstructure modification by adding secondary phases at the intergranular boundaries during processing [7, 8]. Although MgO or Fe_2O_3 as stabilising additives and $MgTi_2O_5$ as heterogeneous nucleation agents could enhance the formation of Al_2TiO_5 solid solutions at a low temperature by a classical solid phase reaction, effectively stabilising the crystal structure and depressing its medium-temperature thermal decomposition, the thermal expansion of the as-received samples usually becomes bigger [3, 9, 10-14]. In the case of the addition of secondary phases, such as mullite, ZrO_2 and Al_2O_3, or the in situ formation of mullite through the addition of SiO_2, though the presence of these reinforced secondary phases may produce a duplex microstructure and restrict the microcrack development as well as improving the mechanical properties of the bulk material, these phases usually have a high thermal expansion coefficient, conferring a slight detrimental effect on its thermal expansion behaviour [4, 6, 7, 15].

Recently, several attempts have been made to improve the mechanical performances and further reduce the thermal expansion coefficient of AT by adding composite additives or by preparing AT-based complex-phase ceramics using natural mineral materials [2, 16-18]. Chen et al. [19] prepared a stable porous Al_2TiO_5-mullite composite ceramics by optimizing the Fe_2O_3, SiO_2, and CaO components in coal fly ash, and found that the CaO and SiO_2 could react with alumina to produce anorthite liquid phase at the grain boundaries, which could accelerate the reaction diffusion and reduce the sintering temperature. Li et al. [20] found that the

thermal stability of Al_2TiO_5 could be enhanced in a silica liquid yielded from the mullitisation of andalusite, which facilitated the sintering and densification of mullite-Al_2TiO_5 composites. Takahashi et al. [21] reported that AT ceramics doped with alkali feldspar exhibited an extremely low thermal expansion coefficient, high sinterability and high thermal stability, high refractoriness, and relatively large fracture strength. Papitha et al. [22] claimed that adding magnesium silicate in pure AT sample could increase the content of Al_2TiO_5 phase, significantly retard the eutectoid decomposition of Al_2TiO_5 phase and thermodynamically stabilize it at elevated temperatures, leading to a significant decrease in the coefficient of thermal expansion.

Porcelain clay contains several commonly reported additives and precursors of mullite reinforcement for the preparation of AT ceramic materials. AT/porcelain ceramics with a dense structure have also been prepared with various compositions [23]. In our preliminary studies, it was found that the addition of MgO-ZnO-Fe_2O_3 composite additives and traditional porcelain clay in the mixture favoured the in situ formation of AT and its yield efficiency at a low sintering temperature. The prepared AT-based ceramics showed a high flexural strength of 48.87 − 86.21 MPa and a high apparent porosity being more than 13.81 %. Calcium oxide is one of the commonly used fluxing mineral compositions in ceramic materials, unfortunately, the effect of the CaO additive on the thermal-mechanical behaviours of AT-based materials have rarely been put forth up to now, and there are still many unsolved questions about the stabilisation mechanism of AT and its reinforcing method. In view of the above, the study aimed to develop AT-based ceramics with both low thermal expansion coefficients and excellent mechanical properties. An innovative synthesis route was applied to produce the AT-based ceramics at a low temperature by an in situ solid-state reaction using MgO-ZnO-CaO system additives and traditional porcelain clay. It can be expected to provide a new cost-effective route to prepare AT-based ceramics.

EXPERIMENTAL

In the present study, industrial titanium dioxide (> 98 %, d50 = 0.2 − 0.3 μm) and aluminium oxide (> 98.5 %, d50 = 8.69 μm) were selected as the raw materials for the synthesis of AT at an equimolar ratio of Al_2O_3–TiO_2. Analytically pure MgO, Fe_2O_3, ZnO, and CaO were used as the composite additives, and traditional porcelain clay produced using kaolin, quartz, and potassium feldspar (Chaozhou, Guangdong, China) (see Table 1) was used to modify the phase composition and improve the densification of the ceramics. Herein, the AT raw materials were milled with the porcelain clay at a mass percentage of 8:2 using a planetary mill for 2 hr, in which 5 wt. % MgO, 3 wt. % Fe_2O_3, and 2 wt. % ZnO were added based on the AT raw materials, respectively, and the amount of CaO changed in a mass proportion of 0, 2, 3, 4, 5 wt. % (hereafter, these mixtures are denoted C0, C2, C3, C4, and C5, respectively). The resulting mixture was pressed at 80 MPa into 38 mm × 6 mm × 6 mm specimens. After drying at 110 ℃, the formed samples were finally sintered in air at 1350 ℃ − 1400 ℃ for 1 h.

Table 1. Chemical composition of porcelain clay (wt. %).

Components	Al_2O_3	SiO_2	Fe_2O_3	CaO	MgO	KNaO	TiO_2	Total
Content	21.99	74.38	0.24	0.26	0.62	2.46	0.05	100

The bulk density and porosity of the obtained samples were evaluated using Archimedes' method. The flexural strength before and after water quenching from 600 ℃ to ambient temperature was examined by a three-point bending test using a universal testing machine. The thermal expansion coefficient was examined with a thermal dilatometer (DIL402, Netzsch, Germany) within a temperature range of 20 − 900 ℃ at a heating rate of 10 ℃·min^{-1}. The microstructures of the samples were observed using a field emission scanning electron microscopy (FE-SEM) (Quant 450FEG, FEI, Hilsboro, USA), and energy dispersive X-ray spectroscopy (EDS) (LE350 Penta FETX-3, Oxford, UK) was also used to analyse the elemental compositions and their distribution on the fracture sample surface. The phase composition was characterised using X-ray powder diffraction (XRD) (AXS D8 Advanced, Bruker, Germany) in the range of $2\theta = 10° - 70°$ with Cu-Kα radiation ($\lambda = 0.154$ nm), and the change in the phase composition was qualitatively evaluated using the peak height intensity ratios from the XRD patterns. Thermal shock tests were performed by water quenching from 600 °C to ambient temperature for three test cycles, and the thermal shock resistance was evaluated by the residual flexural strength after three thermal cycles and the thermal expansion coefficient.

RESULTS AND DISCUSSION

Change in the phase composition

Figure 1 shows the XRD patterns of the C0-C5 samples sintered at 1380 ℃ for 1 h and the C3 sample sintered at various temperatures for 1 h. The main phase of the samples sintered both at 1380 ℃ and at various temperatures was identified as an Al_2TiO_5 solid solution, with a small amount of corundum and newly formed crystal phases. For the C0 sample, gahnite ($ZnAl_2O_4$) and mullite phases were clearly visible. While the secondary crystal phases in the C2-C5 samples were anorthite ($CaAl_2Si_2O_8$), corundum, gahnite, and a magnesium aluminium spinel, no detectable mullite phase was found from the obtained XRD patterns. This is in line with the findings of Chen et al. [19]. The newly formed anorthite and gahnite phases were attributed to the reaction of CaO

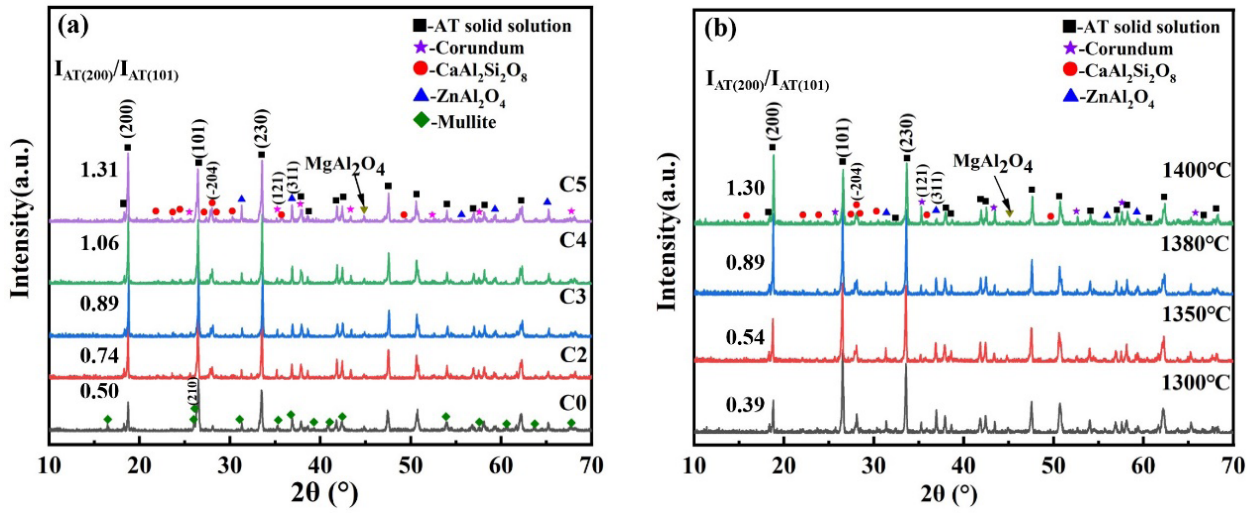

a) C0-C5 samples sintered at 1380 °C

b) C3 sample sintered at different temperatures

Figure 1. XRD pattern of samples sintered for 1 h.

with the Al_2O_3 and SiO_2 in the clay materials and ZnO with Al_2O_3 in the composition, respectively. The addition of CaO showed a great effect on the formation of the anorthite phase, it obviously restricted the production of the mullite phase during the calcining process in comparison with the sample without CaO.

It can be also seen from Figure 1 that the diffraction peak intensity assigned to the Al_2TiO_5 solid solution for the C2-C5 samples was significantly stronger than that for the C0 sample. The strongest diffraction peak gradually changed from a (101) plane to a (200) plane with an increase in the CaO content, but remained a small change in the (230) crystal plane. The peak intensity ratio of the (200) and (101) planes ($I_{AT\,(200)}/I_{AT\,(101)}$, hereinafter) increased from 0.50 to 1.31, which indicated that the crystal growth of the Al_2TiO_5 solid solution showed an oriented growth tendency along the c-axis.

To compare the change of the phase composition, Table 2 shows the diffraction intensity ratio of the strongest peak of each phase that appeared in the sample based on that of the (230) plane of the Al_2TiO_5 solid solution. As for the new formed secondary phase, the diffraction intensity for the anorthite phase became more acute with the addition of CaO, with an intensity ratio of $I_{anorthite\,(\bar{2}04)}/I_{AT\,(230)}$ from 0.13 to 0.21, while the $I_{gahnite\,(311)}/I_{AT\,(230)}$ increased gradually from 0.18 to 0.28. However, only the content of the corundum phase decreased gradually when increasing the CaO amount, showing a value of $I_{corundum(311)}/I_{AT\,(230)}$ decreasing from 0.12 to 0.07. Considering the diffraction intensity changes in the (101), (200), and (230) crystal planes of the Al_2TiO_5 solid solution, together with the changes in the ratios of $I_{anorthite\,(\bar{2}04)}/I_{AT\,(230)}$ and $I_{gahnite\,(311)}/I_{AT\,(230)}$, it can be seen that the addition of CaO in the composition not only promoted the formation of Al_2TiO_5 solid solution and the orientation growth along the c-axis of the crystal to a certain extent, but also improved the relative content of the anorthite and gahnite phases in the samples.

Figure 1b presents the XRD patterns of the C3 sample after being sintered at 1300 °C − 1400 °C for 1 h, no significant change in the phase composition occurred, but the $I_{AT\,(200)}/I_{AT\,(101)}$ increased from 0.39 to 1.30 with an increase in the temperature, and the ratios of $I_{anorthite\,(\bar{2}04)}/I_{AT\,(230)}$ and $I_{gahnite\,(311)}/I_{AT\,(230)}$ decreased from 0.26 to 0.20 and from 0.33 to 0.09, respectively. While the relative content of the corundum phase gradually

Table 2. Phase composition and the relative peak intensity ratio of the samples.

Sample	Temperature (°C)	Phase	$I_{AT(230)}/I_{AT\,(230)}$	$I_{Anorthite(\bar{2}04)}/I_{AT\,(230)}$	$I_{Corundum(121)}/I_{AT\,(230)}$	$I_{Gahnite\,(311)}/I_{AT\,(230)}$	$I_{Mullite(210)}/I_{AT\,(230)}$
C0		ATss + G + M	1			0.30	0.56
C2		ATss + A + C + G	1	0.13	0.12	0.18	
C3	1380	ATss + A + C + G	1	0.17	0.11	0.18	
C4		ATss + A + C + G	1	0.21	0.05	0.23	
C5		ATss + A + C + G	1	0.21	0.07	0.28	
	1300	ATss + A + C + G	1	0.26	0.14	0.33	
C3	1350	ATss + A + C + G	1	0.21	0.08	0.24	
	1400	ATss + A + C + G	1	0.20	0.29	0.09	

note: ATss - Al_2TiO_5 solid solution; A - Anorthite; G - Gahnite; C - Corundum; M - Mullite

increased, showing a value change of $I_{corundum\ (121)}/I_{AT\ (230)}$ from 0.14 to 0.29. Thus, it can be seen that increasing the sintering temperature favoured the formation and orientated growth of the Al_2TiO_5 solid solution along the c-axis, as well as the increase in the corundum phase content and the decrease in the gahnite content in the sintered samples. The amount of anorthite was mainly related to the addition of CaO in the batch composition.

Figure 2 and Table 3 show the SEM image of the C3 sample prepared at 1380 °C and its EDS analysis results. The point scanning analysis results indicated that the long columnar crystal located at point 1 and the massive crystals at point 2 and point 3 were assigned as the Al_2TiO_5 solid solution, and some Mg and Fe elements and extremely small amounts of Ca, Zn, Si elements were also detected in these crystals, which further confirmed that the metal ions introduced through both the added additives and the porcelain clay mainly entered the crystal structure of the Al_2TiO_5 solid solution or formed the glass phase. The small granular crystal at point 4 was identified as the corundum phase was located at the microcracks, and the massive grains at point 5 and the irregular crystal at point 6 were also identified as $ZnAl_2O_4$ & $MgAl_2O_4$ and anorthite. The EDS analysis results also further confirmed the phase composition analysis results examined by XRD.

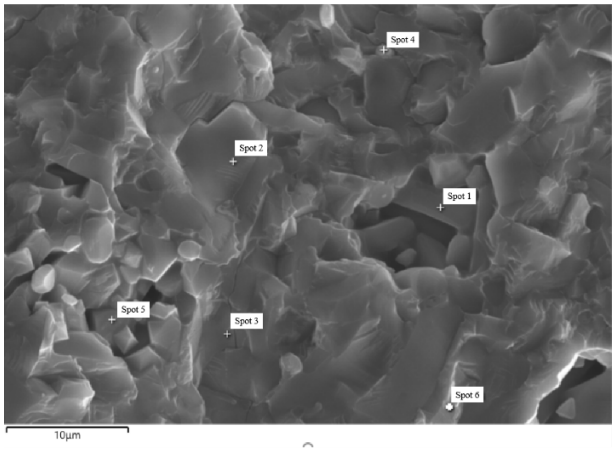

Figure 2. EDS analysis pattern of the C3 sample prepared at 1380 °C.

Changes in the porosity and bulk density

The changes in the bulk density and porosity of the prepared samples in response to the CaO contents and the sintering temperatures are depicted in Figure 3. Increasing the sintering temperature was helpful to improve the bulk density and reduce the porosity, especially for the CaO-free samples. Meanwhile, the addition of CaO could significantly improve the densification of the samples, being in line with the previously reported behaviour [19]. The obtained samples showed a porosity of 5 − 10 % and a bulk density of 3.1 − 3.2 g·cm^{-3} when the CaO content was in the range of 2 − 5 wt. %.

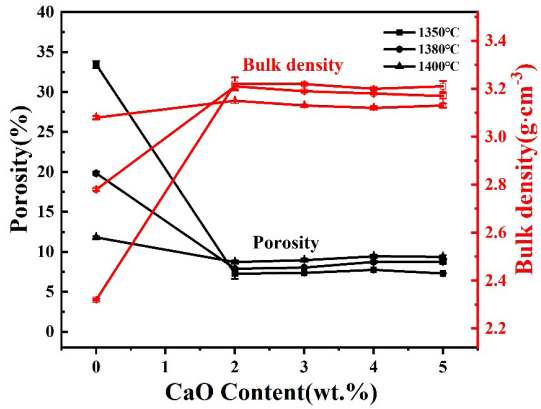

Figure 3. Bulk density and porosity of the AT-based multiphase ceramics.

As is known, CaO is a commonly-used fusing oxide component in traditional ceramic materials, and the densification degree of the samples could be greatly accelerated due to the formation of the liquid phase through a low eutectic reaction at a low temperature [24]. As indicated in the section above, both the addition of CaO in the composition and the increase in the sintering temperature could enhance the formation of the Al_2TiO_5 solid solution. The microcracks caused by the anisotropy of the Al_2TiO_5 solid solution easily decreases the densification of ceramics. Thus, the changes in the bulk density and porosity of the prepared samples were closely associated with the densification degree of the samples and the formation efficiency of the

Table 3. EDS analysis results of the C3 sample prepared at 1380 °C.

Spot	Elemental composition (At. %)								phase
	Al	Ti	Ca	Zn	Si	Mg	Fe	O	
1	18.56	15.64	0.11	0.19	0.28	1.30	1.28	62.64	ATss
2	22.39	16.48	0.08	0.20	0.16	1.23	1.32	58.15	ATss
3	24.00	8.33	0.24	1.49	0.93	3.79	0.82	60.42	ATss
4	30.39	2.14	0.75	0.07	2.01	0.35	0.27	64.02	Corundum
5	43.96	1.46	0.07	13.53	0.74	11.20	1.74	27.31	$ZnAl_2O_4$ & $MgAl_2O_4$
6	16.46	6.20	3.54	0.08	11.05	0.90	0.48	61.29	$Ca(Al_2Si_2O_8)$

Al_2TiO_5 solid solution. The increase in the porosity and the decrease in the bulk density with the increase of CaO content or the increase in sintering temperature led to the overall bulk density being close to the theoretical bulk density of Al_2TiO_5 at 83.7 − 86.5 %.

Mechanical properties and thermal shock resistance

Figure 4 shows the changes in the flexural strength of the AT-based ceramics and the residual strength after water quenching from 600 °C to ambient temperature for 3 cycles. Both the sintering temperature and the addition of CaO showed an obvious effect on the flexural strength. For the samples without CaO, the flexural strength before the water quenching increased from 44.3 to 61.9 MPa with the firing temperature. As indicated in Figure 1 and Figure 3, the marked enhancement of the flexural strength was mainly attributed to the increasing densification through the liquid phase sintering and the mullitisation in the samples.

However, the flexural strength of the C2-C5 samples decreased overall with an increase in the firing temperature, despite the value measured at room temperature ranging from 40.9 MPa to 69.5 MPa when the CaO content was over 2 wt. %. All of these changes were mainly attributed to the existence of microcracks caused by the anisotropic expansion along each crystal axis of the Al_2TiO_5 solid solution. On the other hand, owing to the mismatch of the thermal expansion coefficient between the Al_2TiO_5 crystals and the second phase, such as anorthite ($\alpha = 4.8 \times 10^{-6}$ °C^{-1}), and the gahnite phase ($\alpha = 6.8 \times 10^{-6}$ °C^{-1}) [5, 25 - 26], the compressive residual stress would develop on the surface of Al_2TiO_5 solid solution particulates, by which the thermal decomposition of Al_2TiO_5 solid solution and the microcrack propagation were greatly inhabited, effectively improving the densification degree and mechanical properties. Thus, the strengthening mechanisms in the presence of CaO in the composition were speculated to be the doping mechanism of the reinforcing secondary phase and the extrusion strengthening between the different crystal phases.

Figure 4b illustrates the changes in the residual flexural strength of the samples after water quenching. The strength loss rate of the samples decreased with an increase in sintering temperature and CaO content, but the residual strength was above 30 MPa when the CaO content was 4 − 5 wt. %, especially in the case of the sintering temperature being over 1350 °C, the residual flexural strength could reach 53 − 68 MPa, being greatly higher than that before water quenching. The enhanced performance of the samples after the thermal shock test was attributed to the decrease in the number of microcracks caused by the increase in the thermal stability of the Al_2TiO_5 solid solution and the squeezing effect of newly formed anorthite and gahnite phases on the Al_2TiO_5 solid solution grains.

Figure 5 shows the FE-SEM images of the fracture section of the C3 sample sintered at 1300 − 1400 °C for 60 min. Radial, square and fine granular crystals (Figure 5a) as well as glass-like substances could be seen in the sample prepared at 1300 °C, and only a small number of pores and cracks could be found. However, the small number of microcracks and pores in the inner and boundary of the Al_2TiO_5 solid solution grains also resulted in higher thermal stress accumulation, which made the sample have poor thermal shock resistance and a higher flexural strength loss rate after the thermal shock during the water quenching. When the sintering temperature rose to 1350 − 1400 °C, lamellar and columnar crystals located between the large crystals were observed (Figure 5b-5d), and they were interlocked with each other, conferring a compact structure, which was in line with the XRD analysis and physical-mechanical examination results and previous research findings [19, 21]. Ohya et al. [27] found that liquid-phase sintering occurring during the preparation of Al_2TiO_5 could give rise to

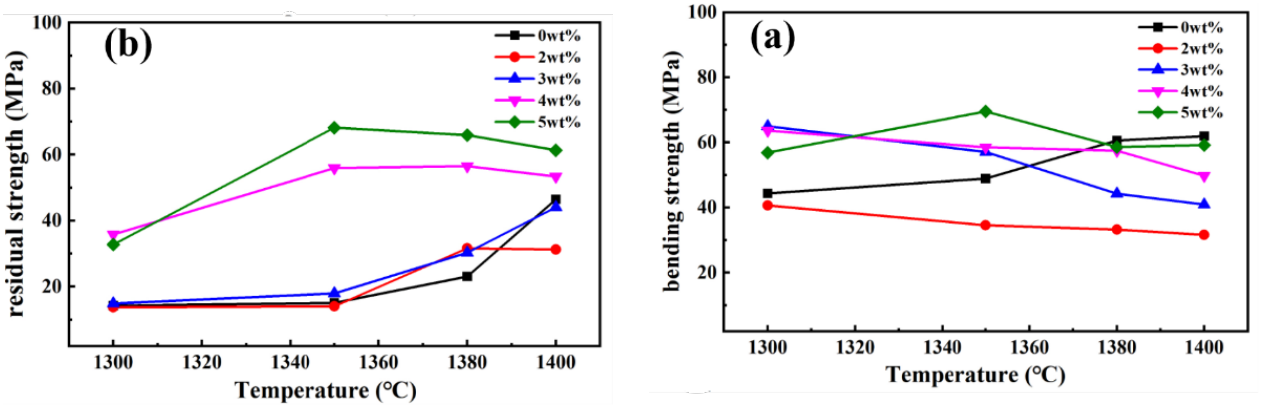

a) before b) after

Figure 4. Flexural strength of the AT-based ceramics before and after water quenching from 600 °C to ambient temperature for 3 cycles.

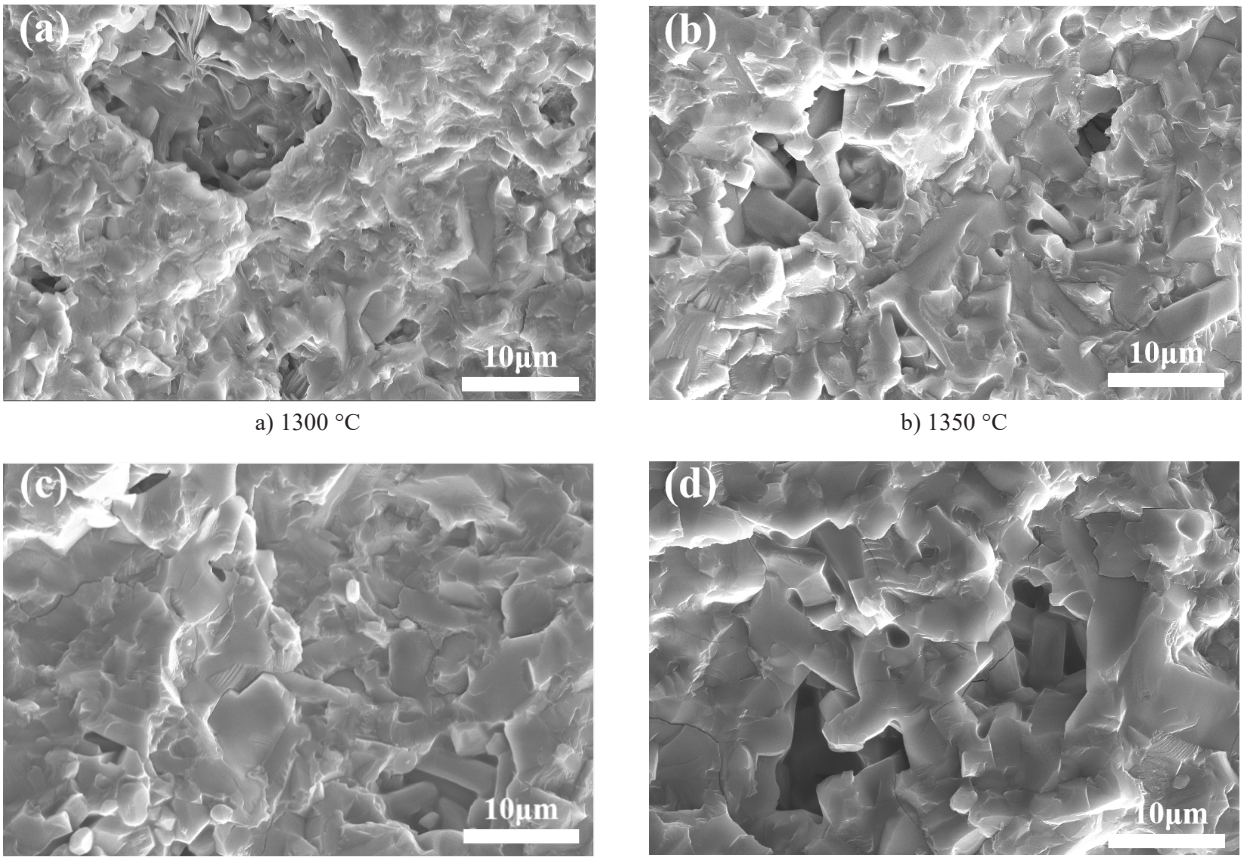

a) 1300 °C b) 1350 °C

c) 1380 °C d) 1400 °C

Figure 5. FE-SEM micrographs of the fractured surface of the C3 samples prepared at different temperatures for 1 h.

elongated Al_2TiO_5 grains through Ostwald ripening. Such a self-reinforced micro-structure effectively prevented the crack propagation and extension, making the obtained ceramics have a high mechanical strength and a very low thermal expansion coefficient. Moreover, the grain pull-out and bridging mechanisms as well as the crack deflection and crack branching caused by the lamellar and columnar crystals also contributed to the observed high mechanical resistance against the crack propagation.

Figure 6 shows the cross-section SEM morphology of the C0, C3, and C5 samples fired at 1380 °C. Many small irregular flake crystals and a large number of connected pores could be found in the FE-SEM images of the C0 sample. Although these small crystals made the number of cracks reduce, the high porosity made

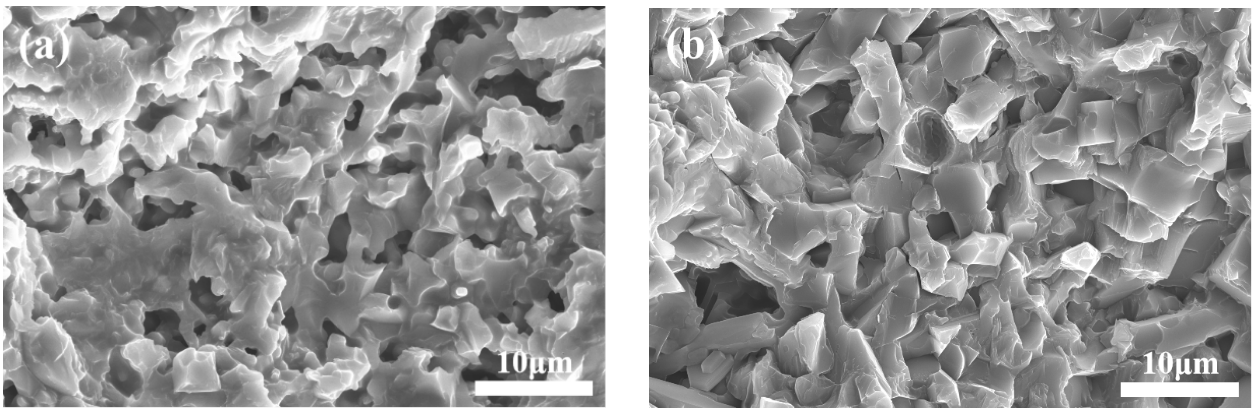

a) C0 b) C5

Figure 6. FE-SEM micrographs of the fractured surfaces of the samples prepared at 1380 °C for 1 h after water quenching for three times from 600 °C to ambient temperature.

continues on the next page ...

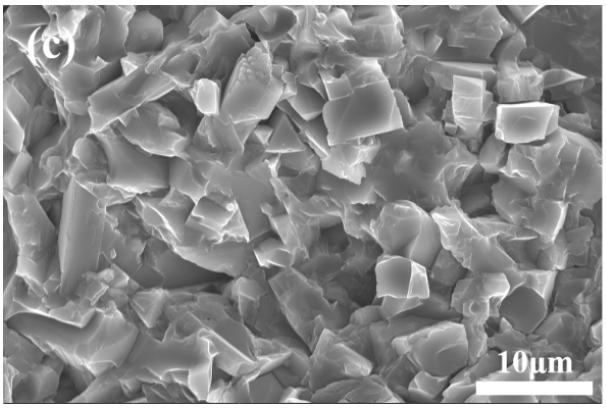

c) C5

Figure 6. FE-SEM micrographs of the fractured surfaces of the samples prepared at 1380 °C for 1 h after water quenching for three times from 600 °C to ambient temperature.

the flexural strength of the samples to become worse (Figure 4 and Figure 7). Whereas, for the samples with the addition of CaO, only small pores could be found and the long columnar grains were also bigger than those in the C0 sample. These long columnar Al_2TiO_5 solid solution crystals in the C5 sample made them easier to overlap with each other, and microcracks also appeared both in the crystal and between the grain boundaries. Figure 6d shows the cross-section of the C5 sample after water quenching for three times. The microcracks between the grains or within the grains were found to be reduced, which might be caused by the microcracks absorbing the strain energy generated during the thermal shock test. Such self-healing of these microcracks made the residual flexural strength to be, on the contrary, enhanced after the water quenching.

Thermal expansion behaviour

Figure 7 shows the changes in the thermal expansion coefficient of the C3 sample obtained at various sintering temperatures and of those with the different CaO contents. The thermal expansion coefficient decreased with both the increase in the sintering temperature and the CaO contents. For the C3 sample, it obviously decreased from 3.99×10^{-6} °C^{-1} to 0.80×10^{-6} °C^{-1} with an increase in the temperature. In the case of the samples with the various CaO additions, the average thermal expansion coefficient at 20 °C − 800 °C decreased from 5.18×10^{-6} °C^{-1} to 0.97×10^{-6} °C^{-1} with an increase in the amount of CaO. When the CaO content was more than 4 wt. %, the thermal expansion coefficients did not show a continuous decrease, which might be related to the increase in the content of the corundum crystal phase in the ceramics. Thus, such a decrease was directly correlated with the formation of the Al_2TiO_5 solid solution and its continuous crystal growth as well as the change in the phase composition during the process.

Usually, the thermal expansion coefficient of ceramic materials is mainly affected by the content of each phase component in the material and their thermal expansion properties. As shown in Figure 1, the phase composition of the samples containing CaO was composed of an Al_2TiO_5 solid solution, anorthite, gahnite, magnesium aluminium spinel, and a small amount of corundum, and the relative content of the Al_2TiO_5 solid solution phase increased with both the increasing temperature and the additional CaO content. Compared with the C0 sample, due to anorthite and gahnite crystals having a lower thermal expansion coefficient than mullite and high thermal stability, such a phase composition effectively conferred the AT based ceramics with a low thermal expansion coefficient. Ohya et al. [27] pointed out that there was a certain relationship between the thermal

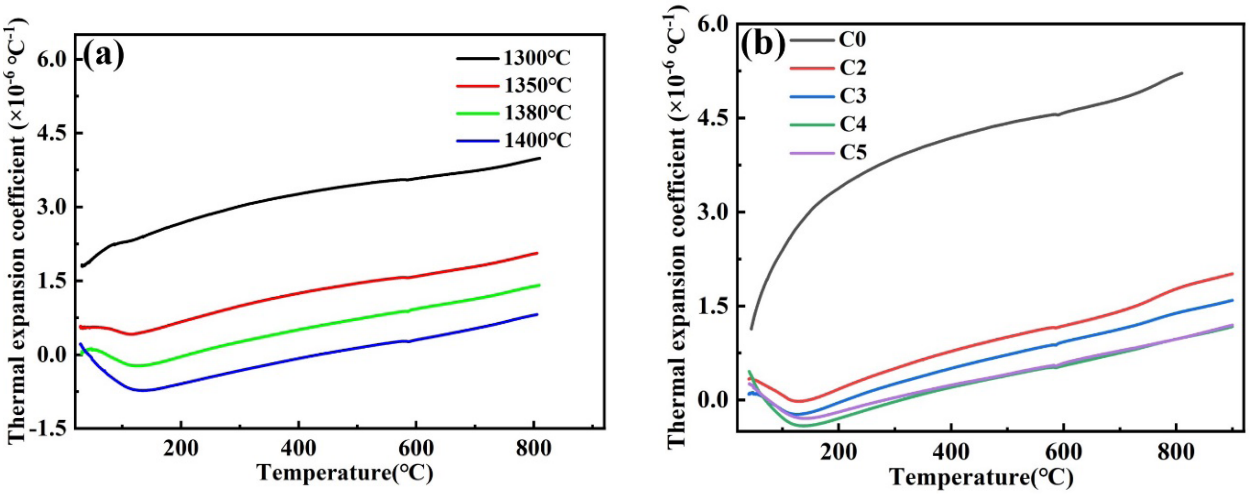

a) C3 sample sintered at 1300 - 1400 °C

b) C0 - C5 samples sintered at 1380 °C

Figure 9. Changes in the thermal expansion coefficient of the AT-based ceramics sintered for 1 h.

expansion coefficient of Al_2TiO_5 ceramics and the content of the microcracks at the crystal boundary. An increase in the microcracks was beneficial to the decrease in the thermal expansion coefficient of Al_2TiO_5 ceramics. Thus, the changes in the phase composition and the formation of the Al_2TiO_5 solid solution easily resulted in a big decrease in the thermal expansion coefficient.

It could be seen from Figure 5 that the microcracks in the ceramics were obviously visible and increased with the sintering temperature. The cylindrical Al_2TiO_5 solid solution crystals were surrounded by anorthite and gahnite crystals in the cross-section of the samples, and bore a squeezing effect exerted by the anorthite crystals and gahnite crystals during the cooling process. Such a microstructure was not only beneficial to increasing the flexural strength of the ceramics, but also effectively prevented the thermal decomposition of Al_2TiO_5 solid solution crystals. In addition, the corundum grains located between the Al_2TiO_5 solid solution grains also exerted a pinning effect on the microcracks, promoting the flexural strength of the ceramics. Thus, the AT-based ceramic composites possessed a low thermal expansion coefficient and a high flexural strength with an increase in the temperature and CaO content.

CONCLUSIONS

AT-based ceramics were successfully synthesised by an in situ solid-state reaction of 20 wt. % porcelain clay and 80 wt. % AT materials. The thermo-mechanical properties of AT-based ceramic materials could be effectively improved with the addition of MgO-ZnO-CaO system complex additives and traditional porcelain clay. The obtained AT-based ceramics exhibited low porosities, large grain sizes, high flexural strengths after sintering, and high retained strengths after the thermal shock tests. The enhanced flexural strength and thermal expansion resistance of the AT-based ceramics were mainly due to the high densification and the changes in both the phase composition and the microstructure. The compressive residual stress developed on the surface of the Al_2TiO_5 solid solution particulates by the mismatch of the thermal expansion coefficient between the Al_2TiO_5 solid solution crystals and the second phases made the Al_2TiO_5 solid solution particulates have a high thermal stability. The formation efficiency of the Al_2TiO_5 solid solution could be enhanced by the addition of CaO in the composition and the increase in the sintering temperature, the resulting microcracks would further reduce the thermal expansion coefficient of the material. The average thermal expansion coefficient of the sample with 3 wt. % CaO was 0.80×10^{-6} °C^{-1} at 20 − 800 °C with a strength of 40.91 MPa, and the flexural strength of the sample with 5 wt. % CaO sintered at 1380 °C could reach 58.59 MPa having a high thermal shock resistance.

Acknowledgment

This work was supported by the Innovation development special foundation of Jieyang science and Technology Bureau, Guangdong, China (No. 2019068).

REFERENCES

1. Ewais E M M, Besisa N H A, Ahmed A. (2017): Aluminum titanate based ceramics from aluminum sludge waste. *Ceramics International, 43*(13), 10277-10287. doi: 10.1016/j.ceramint.2017.05.057
2. Zhao G, Bai Y, Qiao L. (2016): Aluminum titanate-calcium dialuminate composites with low thermal expansion and high strength. *Journal of Alloys and Compounds, 656*, 1-4. doi: 10.1016/j.jallcom.2015.09.237
3. Rezaie H R, Naghizadeh R, Farrokhnia N, Arabi S, sobhani M. (2009): The effect of Fe_2O_3 addition on tialite formation. *Ceramics International, 35*(2), 679-684. Doi: 10.1016/j.ceramint.2008.02.009
4. Tsetsekou A. (2005): A comparison study of tialite ceramics doped with various oxide materials and tialite–mullite composites: Microstructural, thermal and mechanical properties. *Journal of the European Ceramic Society, 25*(4), 335-348. doi: 10.1016/j.jeurceramsoc.2004.03.024
5. Ono T, Sawai Y, Ikimi M, Obata S, Sakurada O, Hashiba M. (2007): Acoustic emission studies of low thermal expansion aluminum-titanate ceramics strengthened by compounding mullite. *Ceramics International, 33*(5), 879-882. doi: 10.1016/j.ceramint.2006.01.005
6. Kornaus K, Lach R, Szumera M, Świerczek K, Gubernat A. (2019): Synthesis of aluminum titanate by means of isostructural heterogeneous nucleation. *Journal of the European Ceramic Society, 39*(7), 2535-2544. doi: 10.1016/j.jeurceramsoc.2019.02.021
7. Perera F H, Pajares A, Meléndez J J. (2011): Strength of aluminum titanate/mullite composites containing thermal stabilizers. *Journal of the European Ceramic Society, 31*(9), 1695-1701. doi: 10.1016/j.jeurceramsoc.2011.03.012
8. Kim I J, Gauckler L G. (2012): Formation, decomposition and thermal stability of Al_2TiO_5 ceramics. *Journal of Ceramic Science and Technology, 3*(2), 49-59. doi: 10.4416/JCST2011-00049
9. Zhang Y, Yin Y. (2000): An initial study on SiCw-reinforced Al_2TiO_5 composites. *Materials Letters, 46*(2), 147-148. doi: 10.1016/S0167-577X(00)00158-0
10. Buscaglia V, Nanni P, Battilana G, Aliprandi, Carryd C. (1994): Reaction sintering of aluminum titanate: I—effect of MgO addition. *Journal of the European Ceramic Society, 13*(5), 411-417. doi: 10.1016/0955-2219(94)90018-3
11. Guedes-Silva C C, Carvalho F M d S, Ferreira T S, Genova L A. (2016): Formation of aluminum titanate with small additions of MgO and SiO_2. *Materials Research, 19*, 384-388. doi: 10.1590/1980-5373-MR-2015-0498
12. Buscaglia V, Delfrate M A, Leoni M, Bottino C, Nanni P. (1996): The effect of $MgAl_2O_4$ on the formation kinetics of Al_2TiO_5 from Al_2O_3 and TiO_2 fine powders. *Journal of materials science, 31*(7), 1715-1724. doi: 10.1007/BF00372183
13. Korim T. (2009): Effect of Mg^{2+}- and Fe^{3+}- ions on formation mechanism of aluminum titanate. *Ceramics International,*

35(4), 1671-1675. doi: 10.1016/j.ceramint.2008.07.017
14. Huang Y X, Senos A M R, Baptista J L. (1998): Effect of excess SiO_2 on the reaction sintering of aluminum titanate–25 vol. % mullite composites. *Ceramics International, 24*(3), 223-228. doi: 10.1016/S0272-8842(97)00006-0
15. Violini M A, Hernandez M F, Gauna M, Suarez G, Conconi M S, Rendtorff N M. (2018): Low (and negative) thermal expansion Al_2TiO_5 materials and Al_2TiO_5-$3Al_2O_3{\cdot}2SiO_2$ - $ZrTiO_4$ composite materials. Processing, initial zircon proportion effect, and properties. *Ceramics International, 44*(17), 21470-21477. doi: 10.1016/j.ceramint.2018.08.208
16. Wohlfromm H, Moya J S, Pena P. (1990): Effect of $ZrSiO_2$ and MgO additions on reaction sintering and properties of Al_2TiO_5-based materials. *Journal of Materials Science, 25*(8), 3753-3764. doi: 10.1007/BF00575415
17. Li J, Yu J, Zhao H, Zhang H. (2022): Ceramic composites based on in situ calcium hexaaluminate/aluminum titanate prepared from ferrotitanate slag. *Materials Today Communications, 31*, 103237. doi: 10.1016/j.mtcomm.2022.103237
18. Ma Q, Shan Q, Chen C, Xu Q, Wang Y, Zhou Y, Shui A. (2022): The influence of ZrO_2 on the microstructure and mechanical properties of Al_2TiO_5 flexible ceramics. *Materials Characterization, 185*, 111719. doi: 10.1016/j.matchar.2022.111719
19. Chen Z, Xu G, Du H, Cui H, Zhang X, Zhan X. (2019): Realizable recycling of coal fly ash from solid waste for the fabrication of porous Al_2TiO_5-mullite composite ceramic. *International Journal of Applied Ceramic Technology, 16*(1), 50-58. doi: 10.1111/ijac.13092
20. Li L, Wang Q, Liao G, Li K, Ye G. (2018): Densification behavior of mullite-Al_2TiO_5 composites by reaction sintering of natural andalusite and TiO_2. *Ceramics International, 44*(4), 3981-3986. doi: 10.1016/j.ceramint.2017.11.191
21. Takahashi M, Fukuda M, Fukuda M, Fukuda H, Yoko T. (2002): Preparation, structure, and properties of thermally and mechanically improved aluminum titanate ceramics doped with alkali feldspar. *Journal of the American Ceramic Society, 85*(12), 3025-3030. doi: 10.1111/j.1151-2916.2002.tb00573.x
22. Papitha R, Suresh M B, Das D, Johnson R. (2013): Effect of micro-cracking on the thermal conductivity and thermal expansion of tialite (Al_2TiO_5) ceramics. *Processing and Application of Ceramics, 7*(3), 143-146. doi: 10.2298/PAC1303143P
23. Sacli M, Onen U, Boyraz T. (2015): Microstructural characterization and thermal properties of aluminum titanate/porcelain ceramic matrix composites. *Acta Physica Polonica A, 127*(4), 1133-1135. doi: 10.12693/APhysPolA.127.1133
24. Zhang L, Zhang W, Zhang J-h, Li G-q. (2016): Effects of additives on the phase transformation, occurrence state, and the interface of the Ti component in Ti-bearing blast furnace slag. *International Journal of Minerals, Metallurgy, and Materials, 23*(9), 1029-1040. doi: 10.1007/s12613-016-1320-2
25. Ballarini A D, Bocanegra S A, Castro A A, Miguel S R, Scelza O A. (2009): Characterization of $ZnAl_2O_4$ obtained by different methods and used as catalytic support of Pt. *Catalysis Letters, 129*(3-4), 293-302. doi: 10.1007/s10562-008-9833-6
26. Cheng X, Ke S, Wang Q, Wang H, Shui A, Liu P. (2012): Fabrication and characterization of anorthite-based ceramic using mineral raw materials. *Ceramics International, 38*(4), 3227-3235. doi: 10.1016/j.ceramint.2011.12.028
27. Ohya Y, Yamamoto S, Ban T, Tanaka M, Kitaoka S. (2017): Thermal expansion and mechanical properties of self-reinforced aluminum titanate ceramics with elongated grains. *Journal of the European Ceramic Society, 37*(4), 1673-1680. doi: 10.1016/j.jeurceramsoc.2016.11.037